On the utility of thermogravimetric analysis for exploring the kinetics of thermal degradation of lignins

Annan Xiang, John R. Ebdon, A. Richard Horrocks, and Baljinder K. Kandola*

Institute for Materials Research and Innovation, University of Bolton, Deane Road, Bolton BL3 5AB, UK

*Corresponding Author: Baljinder K. Kandola, Institute for Materials Research and Innovation, University of Bolton, Deane Road, Bolton BL3 5AB, UK; B.Kandola@bolton.ac.uk; Tel.: +44 1204903517

Abstract

The kinetics of pyrolysis of organosolv (TcA) and hydroxypropyl-modified (TcC) lignins have been investigated using thermogravimetric analysis (TGA). Three isothermal models (single first order, Guggenheim and Avrami-Erofeev) and one non-isothermal model (Kissinger) were used to analyse the mass-loss data. Sensible derived kinetic parameters, i.e., activation energy and pre-exponential factor, were obtained only for the initial stages of pyrolysis where the kinetics were approximately first order. Models that analysed TGA data beyond the initial stage gave inconsistent results, indicating the complexity of subsequent decomposition steps occurring at higher temperatures and/or longer times. The kinetics of the initial stage are important for designing routes to lignin's valorisation into useful products, such as carbon fibres, activated carbons, polymer additives, etc. TcC had a higher activation energy (41.5 kJ/mol) for initial decomposition than TcA (39 kJ/mol), consistent with its greater thermal stability observed previously during conversion of lignin-based fibres into carbon fibres.

Keywords: Lignin, Pyrolysis, Isothermal, Non-isothermal, Thermogravimetry, Kinetics, Activation energy, Pre-exponential factor.

1. Introduction

Lignin is a naturally occurring organic polymer of complex and relatively ill-defined structure. It is major constituent (along with cellulose) of most woody plant species. Lignin has a high carbon content (> 60%) (Gellerstedt and Henriksson, 2008) and excellent char-forming ability (Li et al., 2002; Zhang et al., 2021) when heated, which can be exploited in the development of new products for value-added applications such as carbon fibres, activated carbons, flame retardant additives for other polymers, etc., (Muthuraj et al., 2020; Muthuraj et al., 2021). All of these processes require different heating conditions (temperature, gaseous environment and dwell time) and thermal processing becomes more complex when lignin is blended with other polymers for a particular application. For example, recent work exploring the possibility of carbon fibre production from lignin-based precursor fibres, has shown the latter have to be thermally stabilised in an air atmosphere at a very slow heating rate (usually 0.1 - 0.25 ºC/min) in various stages with different dwell times up to a maximum of 250 ºC, while lignin cross-links, thus changing the thermoplastic property to one of thermosetting (Muthuraj et al., 2021; Culebras et al., 2018a). Thermally stabilised fibre is then carbonised in nitrogen by heating at a high heating rate (e.g., ≥ 20 ºC/min) to 1000 ºC or higher (Muthuraj et al., 2021). Similarly during activated (porous) carbon production, the heating rate and carbonisation temperature are the main controlling factors (Ouyang et al., 2020; Liao et al., 2022).

Chemical structure and properties of the lignin depends upon the type of wood (e.g., softwood or hardwood), method of extraction (e.g., kraft, sulfite, organosolv, steam explosion, etc), molecular weight, degree of branching, purity, etc. (Lupoi et al., 2015). Hence, there can be no simple, single structural representation of lignin. Generically, it is considered to be a cross-linked and highly heterogeneous aromatic polymer (see Scheme 1) comprising syringyl, guaicyl, and *p*-hydroxyphenyl components, the relative contents of which determine the properties of the derived lignin (Lupoi et al., 2015). Owing to its complex chemical structure and complicated pyrolysis pathways involving a range of sequential and parallel reactions, the mechanism of the pyrolysis of lignin is not fully understood (Patwardhan et al, 2011). In anticipating the effects of heating under an inert atmosphere, the weakest and therefore most labile bonds in lignin may be considered to be C-OH, Ar-OH, C-OR and Ph-OR (where R may be-CH_3, -CH_2, -CH, -OH and -CO). It is likely, however, that during extraction and processing, other reactive groups are generated, which in the presence of trace oxidants or oxygen could include peroxy and hydroperoxy species. The presence of trace ionic impurities such as SO_4^{2-}, Fe^{3+}, etc. may also influence the stabilities of these groups in terms of their potential catalytic and redox properties.

An intensive and comprehensive understanding of the pyrolysis of lignin is helpful for the improvement and optimization of products derived from it and the properties of pyrolyzed products (Brebu and Vasile, 2010). Pyrolysis produces solid (char), liquid (tar) and gaseous products. The distribution of these products significantly depends on the pyrolysis conditions such as temperature, heating rate, residence time, etc. Controlled pyrolysis can generate high value-added products such as acetic acid, methanol, charcoal, phenolic compounds (Effendi et al., 2008), carbon fibre (Culebras et al., 2018b; Muthuraj et al., 2020; Muthuraj et al., 2021) and activated carbon (Suhas et al., 2007).

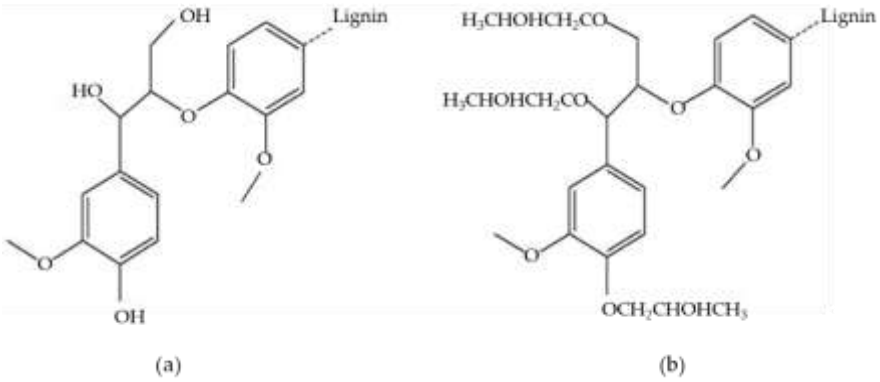

Scheme 1. Simplified chemical structures of (a) organosolv hardwood lignin, TcA and (b) hydroxypropyl-modified lignin, TcC.

Kinetic studies of pyrolysis enable the characterisation of the effects of reaction temperature, reaction time and other parameters on the rates of conversion of reactant to products and the number of reaction steps during thermal decomposition (Narnaware and Panwar, 2022). The sensitivity of reaction processes to temperatures can be better understood by kinetic analysis, in which measurements of rates of reaction (or better rate constants) as a function of temperature and concentration enable determination of kinetic parameters such as order of reaction, apparent activation energy (E_a), and Arrhenius pre-exponential factor (A), although some kinetic analytical methods assume first order kinetics during the initial stages of decomposition (Saddawi et al., 2009). The value of E_a reflects how sensitive the rate of reaction is to temperature changes (Solomons et al., 2017). The greater the value of E_a, the more sensitive is the reaction to changes of temperature and vice versa. A is the temperature-independent component of the rate constant and for simple reactions may represent a frequency of bond vibration or collision between groups required for successful reaction

(Freeman and Carroll, 1958). Thus, these kinetic parameters can provide useful information towards the understanding of the temperature dependence of the reaction processes, hence their valorisation into value-added products.

Thermogravimetric analysis (TGA), in which the mass loss as a function of temperature, or time, of a sample subjected to controlled heating is recorded, is the most commonly used technique for studying the kinetics of thermal degradation of polymers. It should be noted, however, that TGA only gives information about degradation processes leading to mass loss, i.e evolution of volatiles, and therefore not to processes such as crosslinking. Two main TGA-based analytical methods have been used to obtain kinetic parameters: isothermal and non-isothermal. Many methods have been proposed to obtain kinetic parameters from TGA data, which depend not only on experimental conditions but also on the mathematical treatment applied to the data. All kinetic studies based on TGA assume that during the thermal decomposition process, the decomposition rate of solid materials can be described by Eq. (1).

$$\frac{d\alpha}{dt} = k(1-\alpha)^n \qquad (1)$$

In which n is the reaction order and α represents the fraction of solid material remaining at time t, as expressed in Eq. (2),

$$\alpha = \frac{m_0 - m_t}{m_0 - m_f} \qquad (2)$$

where m_0 is the initial mass, m_f represents the final mass at the completion of reaction and m_t is the mass at time t. k is the rate constant and is given by Eq. (3),

$$k = Ae^{\left(\frac{-E_a}{RT}\right)} \qquad (3)$$

where A is the pre-exponential factor, R is the gas constant, E_a is the activation energy and T is the reaction temperature (K). Combining Eq. (1) with Eq. (3), gives Eq. (4):

$$\frac{d\alpha}{dt} = Ae^{\left(\frac{-E_a}{RT}\right)}(1-\alpha)^n \qquad (4)$$

For a linear heating rate, $\beta = \frac{dT}{dt}$, Eq. (4) can be re-written as Eq. (5):

$$\frac{d\alpha}{dT} = \frac{A}{\beta}e^{\left(\frac{-E_a}{RT}\right)}(1-\alpha)^n \qquad (5)$$

Both integral and differential methods have been used to calculate kinetic parameters based on Eq. (5), some examples of the former being Coats-Redfern (Coats and Redfern, 1964) and Flynn-Wall-Ozawa (FWO) methods (Ozawa, 1965, Flynn and Wall, 1966) and for the latter Friedman (Friedman, 2007), Freeman-Carroll (Freeman and Carroll, 1958) and Kissinger (Kissinger, 1957) methods.

Many researchers have studied the pyrolysis kinetics of different lignin types using isothermal (Chan and Krieger, 1981; Ojha et al., 2017; Pasquali and Herrera, 1997) and non-isothermal approaches (Avni and Coughlin, 1985; Ferdous et al., 2002; Hu and Jiang, 2020; Jiang et al., 2010; Mani et al., 2009; Wang et al, 2014) and reported that the parameters depend upon the lignin type, experimental conditions and model used. Many investigators have assumed a single first-order reaction for the thermal decomposition of lignin, but this assumption is almost certainly inappropriate for a complex process such as lignin decomposition, especially after the initial stages have occurred. While some researchers have investigated the kinetic characteristics of lignin decomposition using a single heating rate (Ramiah, 1970; Kumar et al, 2019), others used a series of heating rates (Dash et al., 2022; Wang et al., 2016) as previously suggested by Ozawa (Ozawa, 1965) and Flynn and Wall (Flynn and Wall, 1966), in order to give a better picture of the decomposition process. In addition, the distributed activation energy model (DEAM), has been used to model decomposition over a wide range of temperatures (Mani et al., 2009). In this model, degradation is assumed to be described by a set of first order reactions, for which activation energies at different stages may be calculated.

The aim of present work is to investigate the kinetics of pyrolysis (specifically of thermally induced mass loss) of two types of hardwood lignin (organosolv, TcA and hydroxypropyl-modified, TcC) using both isothermal and non-isothermal thermogravimetric analyses (TGA) that in previous work have been considered to be candidates for carbon fibre precursors (Muthuraj et al., 2020; Muthuraj et al., 2021) and in ongoing work for production of activated carbon. These two lignins have been previously fully characterised for their physico-chemical and thermal degradation properties (Culberas et al., 2018b), and, given that these have been seen to be good candidates for carbon fibre and activated carbon production, are of interest for the present work. Four different kinetic models are applied to the TGA data and the results compared in an attempt to critically evaluate the relative merits and utilities of the models. These studies will complement previous work (Culebras et al., 2018), which studied the temperature-dependent physical and chemical properties, including release of volatiles during pyrolysis of these lignin types. There it was demonstrated that their pyrolysis, although superficially similar, follow significantly different paths at the molecular level, leading to formation of different products.

2. Materials and Methods

2.1 Materials

Unmodified organosolv hardwood lignin (TcA), with an average molecular weight (Mw) of *ca.* 3950 g/mol, a T_g of 100°C, and phenolic hydroxyl (OH_{ph}) group content of 2.4 mmol/g, and a hydroxypropyl-modified lignin (TcC) with Mw of *ca.* 11357 g/mol (Culebras et al., 2018) were both sourced from Tecnaro, Ilsfeld, Germany.

2.2 Thermogravimetry

The thermogravimetric tests were performed on a TA (UK) SDT-Q600 instrument with samples of around 7-9 mg in nitrogen with a flow rate of 100 ml/min.

The isothermal runs were started at the temperature of interest (see Section 2.1) and kept at that temperature for 120 minutes.

For non-isothermal thermogravimetric tests, measurements were started at room temperature (20°C) and ramped to 110°C, held at this temperature for 10 minutes to complete dehydration and then heated further from 110 °C to 900 °C at various heating rates between 5 and 100 °C/min. The TGA results were analysed using the TA Instruments Universal Analysis 2000 software. Each test was repeated three times.

3. Results

3.1. Isothermal kinetic study using single first-order reaction model

The first kinetic model used follows the general isothermal approach in assuming that thermal degradation is a single, simple, first-order reaction from which a single activation energy (E_a) and pre-exponential factor (A) may be derived. This approach consisted of collecting data from six TGA runs conducted isothermally at different temperatures for a fixed duration. The temperatures for isothermal runs were chosen based on the decomposition temperature range of each lignin, determined from dynamic TGA curves. Fig. 1 (a) shows a dynamic TGA graph of the two different lignins used in this work from room temperature to 1200 °C with a heating rate of 20 °C/min. It can be seen that initial mass loss (~5%) occurs over the temperature range 80 - 150 °C; this is due to dehydration of the sample. The main decomposition region of TcA occurs between 240 and 400 °C and between 270 and 410 °C for TcC. Thus, six different temperatures ranging from 240 °C to 350 °C for TcA and 270 °C to 370 °C for TcC were then chosen for the isothermal experiments.

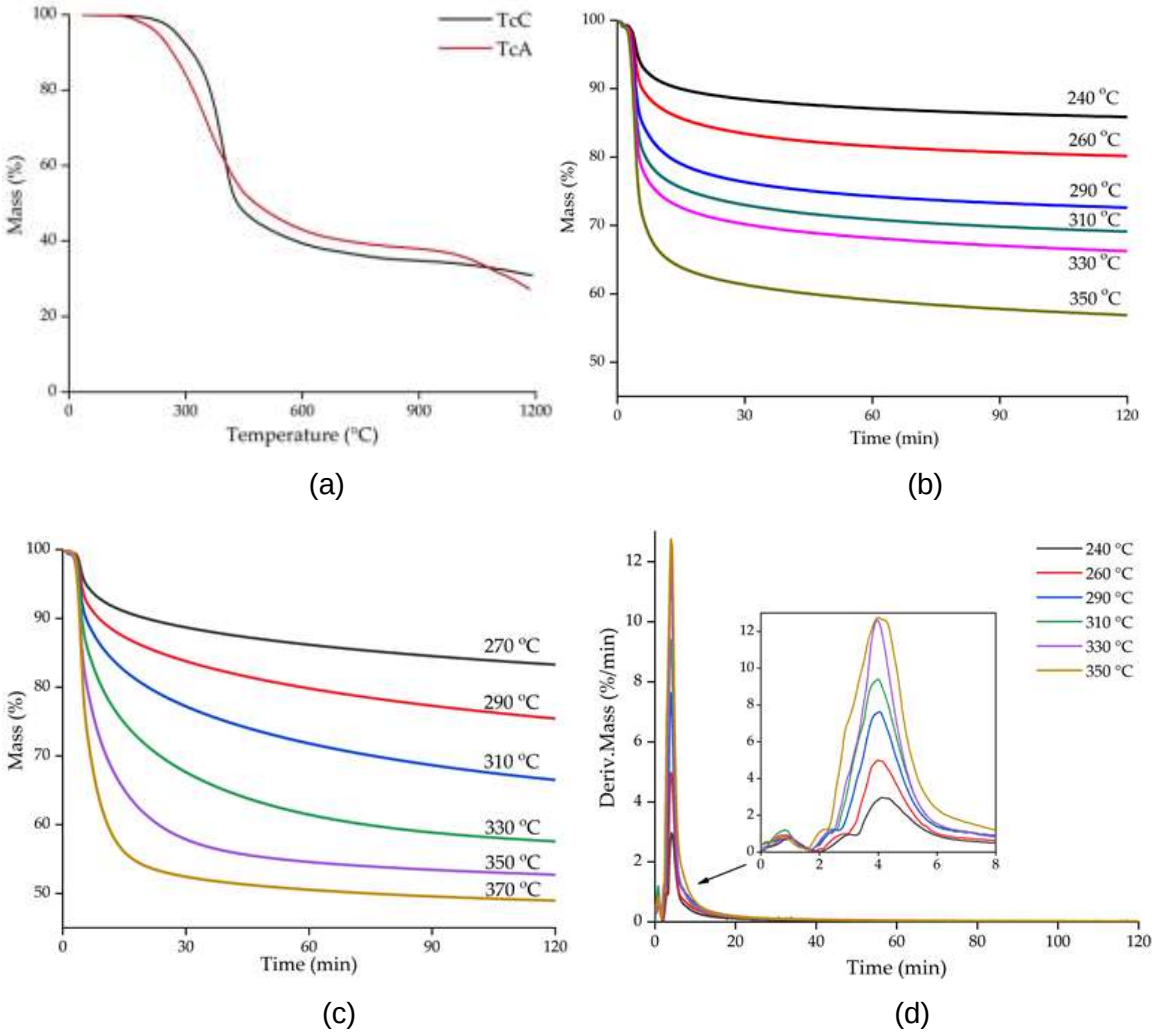

Fig. 1. (a) Dynamic mass loss vs. temperature curves for TcA and TcC lignins;. (b,c) and isothermal mass loss vs. time curves for (b) TcA and (c) TcC at different temperatures; and (d) DTG curves of TcA isothermal runs at six different temperatures under nitrogen.

Isothermal, mass loss vs. time curves at six different temperatures are shown in Fig.1 (b) and (c). Fig. 1 (d) shows DTG curves of TcA isothermal runs under six different temperatures listed in Fig. 1 (b). The small peak at before 3 minutes in Fig. 1 (d) represents the short non-isothermal (stabilisation) period with fast increasing temperature, several seconds over which the temperature stabilises during which water is eliminated prior to thermal degradation commencing.

From these data, the fractional conversion α can be determined using Eq. (6):

$$\alpha = (1 - \frac{m_t}{100}) \qquad (6)$$

where m_t represents the percentage of the mass remaining at any time. Each curve in Fig 1 (b, c) therefore can be defined by Eq. (7):

$$\frac{-d(1-\alpha)}{dt} = k(1-\alpha)^n \qquad (7)$$

where n is the order of reaction, t is the time and k is the rate constant. Assuming thermal degradation is a first order reaction, n =1 and Eq. 7 can be integrated to give Eq. (8):

$$-\ln(1-\alpha) = kt \qquad (8)$$

If the reaction is truly first order, plotting $-\ln(1-\alpha)$ against t, k should give a straight line. An exemplar plot for isothermally degraded TcA at 240 °C is shown in Fig. 2 (a).

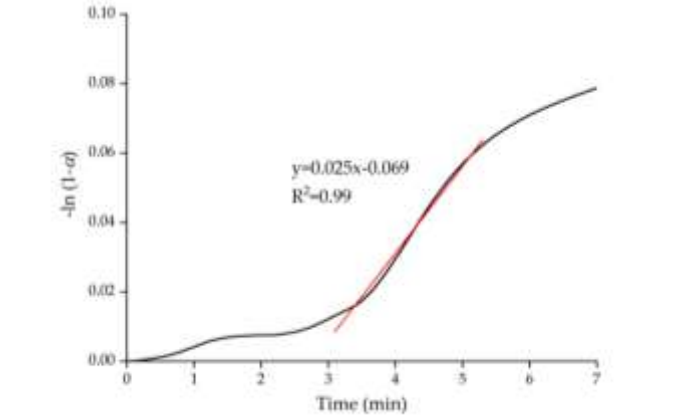

(a)

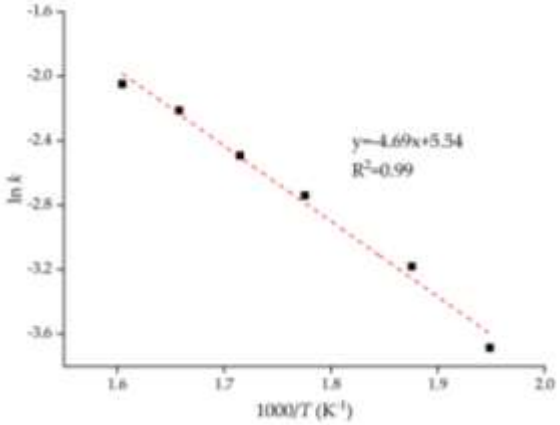

(b)

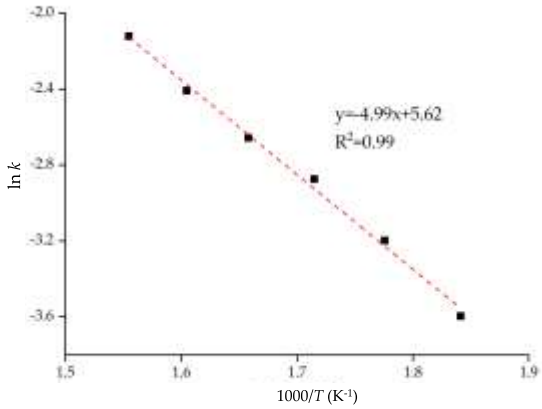

(c)

Fig. 2. (a) Plot of -ln (1-*α*) against *t* for TcA at 240 °C under nitrogen; and Arrhenius plots for TcA (b) and TcC (c) from isothermal initial mass loss data.

The non-linear region during the first 3 minutes in Fig. 1 (b, c) represents the moisture loss occurring both during and immediately after thermal stabilisation. However, even beyond

this stabilisation period, the plot in Fig. 2 (a) is only (approximately) linear during the 3 to 5 minute period, indicating deviation from first order behaviour at higher reaction times as additional reactions occur (Brebu and Vasile, 2010). Thus, in the plot shown in Fig. 2 (a), the rate constant was calculated only from the slope of the curve over the 3-5 min data interval (i.e. from initial rates of mass loss once the temperature had stabilised) using a linear regression procedure. Logarithms of rate constants calculated in this way from mass loss vs. time curves obtained at all the isothermal temperatures were subsequently plotted as a function of the inverse of the absolute temperature (K) (Fig. 2 (b, c)) to give activation energies (E_a) and pre-exponential factors (A) in accordance with the Arrhenius Eq. (9)

$$\ln k = \ln A - \frac{Ea}{RT} \qquad (9)$$

From the data in Fig. 2 (b, c), the activation energies (E_a) for the initial mass loss stages of decomposition of TcA and TcC were calculated to be 39.0 ± 2.0 and 41.5 ± 1.4 kJ/mol, respectively, and the pre-exponential factors (A) to be 256 ± 109 and 277 ± 80 min^{-1}, respectively. The values for both lignins are similar, indicating that the initial stages of pyrolysis for both lignin types are also similar. These values compare favourably with those obtained from isothermal experiments reported by Pasquali and Herrera (1997) (E_a = 12.49 - 42.60 kJ/mol, from TGA experiments), Chan and Krieger (1981) (E_a = 25.2 kJ/mol, $A = 4.7\times10^2$ min^{-1}, from microwave reactor experiments) and Ojha et al (2017) (E_a = 9 - 23 kJ/mol, $A = 1.5\times10^2$ min^{-1}, from Py-FTIR experiments).

3.2 Isothermal kinetic analysis using Guggenheim's method

Since the first-order reaction model applied here considers only the initial rates of reaction as a function of temperature, the application of which is made difficult by the presence of the stabilisation period during which the sample is being heated up and is therefore not isothermal, Guggenheim's method, which also assumes first order reactions but allows the determination of the rate constants without needing to know the initial or final concentrations (or in this case masses), was also used. The Guggenheim method (Guggenheim, 1926), which is a rather neglected but nevertheless useful method for the analysis of kinetic data, is briefly outlined below.

For a first-order reaction, the relation between mass (m) and time (t) can be expressed as:

$$m_t - m_f = (m_0 - m_f)e^{-kt} \qquad (10)$$

where m_t is the mass at time t,

m_f is the mass at the end of reaction,

m_0 is the mass at the beginning of reaction,

k is the rate constant, and

t is the time.

When $t = t + \Delta t$, Eq. (10) becomes:

$$m_{t+\Delta t} - m_f = (m_0 - m_f)e^{-k(t+\Delta t)} \quad (11)$$

Subtracting Eq. (10) from Eq. (11) gives Eq. (12)

$$m_t - m_{t+\Delta t} = (m_0 - m_f)e^{-kt}(1 - e^{-k\Delta t}) \quad (12)$$

Taking logarithms of Eq. (12) leads to

$$\ln(m_t - m_{t+\Delta t}) = -kt + \ln((m_0 - m_f)(1 - e^{-k\Delta t})) \quad (13)$$

By plotting the $\ln(m_t - m_{t+\Delta t})$ against t, the rate constant k can be obtained from the slope. The method relies on measurements of changes in the amount of reactant over a series of fixed time intervals and is thus not dependent on knowing either m_0 or m_f. Comparing rate constants calculated from mass loss vs. time points in the early regions of the plot with those calculated from points obtained later in the reaction allows the identification of any changes in rate constant with degree of conversion. If the rate constant in the early region is different from that in a later region, it indicates that first order kinetics do not apply throughout the reaction, and/or that the activation energy, E_a, and pre-exponential factor, A, vary during the pyrolysis process owing to changes in the types of reaction occurring.

The isothermal TGA curves at various temperatures in Fig. 1 (b, c) show that both lignins decompose at rapid rates at the beginning and then the rates become much lower at longer reaction times, especially after 20 minutes. Before being able to generate $\ln(m_t - m_{t+\Delta t})$ against t plots the time interval Δt needs to be determined for different time ranges. In this work, this was done using a trial-and-error approach such that different Δt values were chosen for different regions of the mass loss vs. time curves so as to give $(m_t - m_{t+\Delta t})$ values that were not vanishingly small; this is a particular problem when mass is changing only very slowly with time at longer reaction times. Fig. 3 (a) shows, as an example, a plot of $\ln(m_t - m_{t+\Delta t})$ against t for TcA at 350 ^{o}C with a time interval Δt of 0.05 min. However, this value of Δt is only appropriate for data collected between about 4.4 and 5.8 min (data before 4.4 min is ignored since in this region, the sample has not yet reached the final isothermal temperature). The slope of the plot decreases rapidly up to 5.8 min, becomes lower after 5.8 min and then much lower after 11 min (not shown in Fig. 3 (a), which means there are more sampling points available

after 5.8 min and even more after 11 min. Thus, two larger Δt values for these second and third stages were required to more accurately determine the assumed first order rate constants applying over these stages. Consequently, the plot of $\ln(m_t - m_{t+\Delta t})$ against t shown in Fig. 3 (a) was divided into three regions covering three different time intervals and replotted as shown in Fig. 3 (b – d).

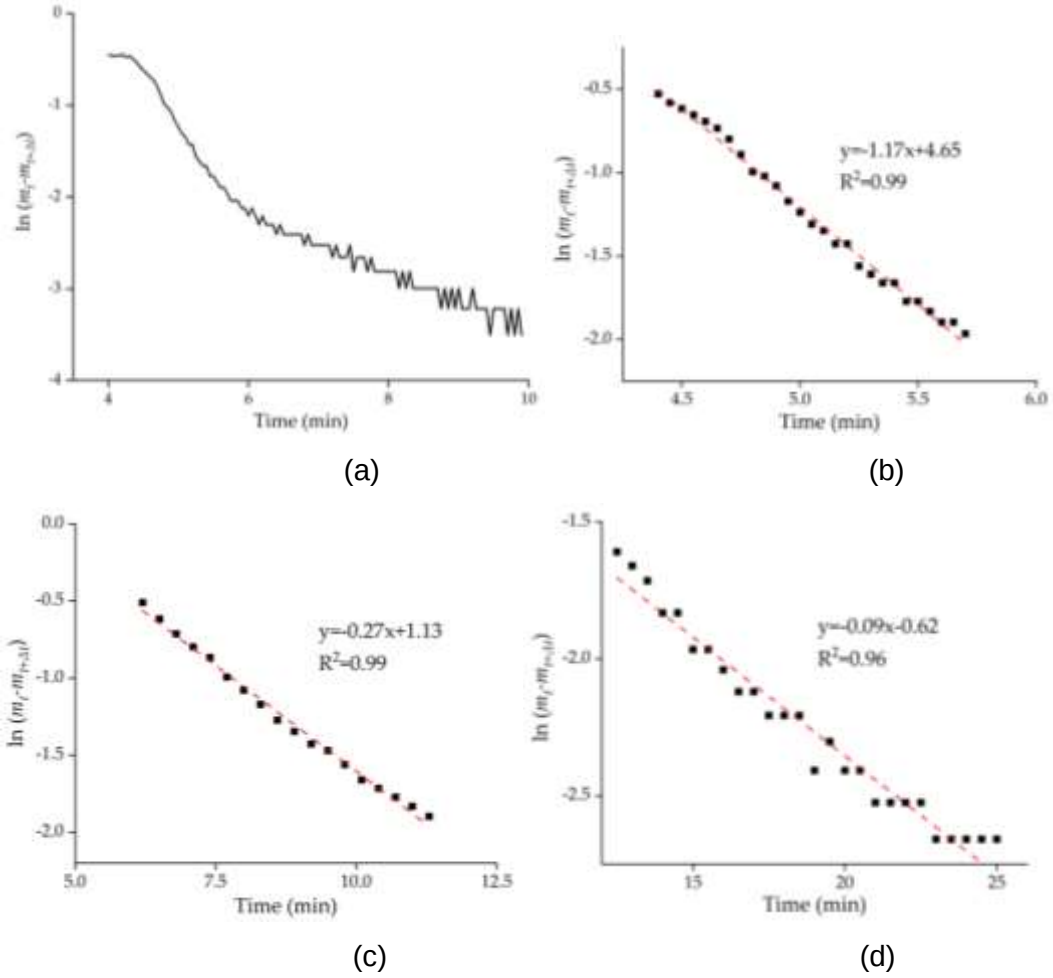

Fig. 3. (a) Plot of ln (m_t-$m_{t+\Delta t}$) vst t of TcA at 350 °C with a time interval, Δt = 0.05 min; and over three different time intervals: (b) 4.4-5.7 min (Δt = 0.05 min), (c) 6.2-11.3 min (Δt = 0.3 min) and (d) 12.5-25 min (Δt = 0.5 min).

From the slopes of these plots, the rate constant k was found to be 1.17, 0.27 and 0.09 min^{-1} for the three different time intervals. These procedures were repeated using the isothermal degradation data for both lignins for all the chosen isothermal temperatures. Tables 1 and 2 list

the complete set of rate constants for TcA and TcC obtained at all temperatures employed and over three different time intervals from the start of reaction.

Table 1. Rate constants obtained for TcA.

T (°C)	*k* (4.4 – 5.7 min)	*k* (6.2-11.3 min)	*k* (12.5-25 min)
240	0.77	0.21	0.1
260	0.86	0.19	0.09
290	1.01	0.18	0.09
310	1.07	0.23	0.07
330	1.11	0.23	0.08
350	1.17	0.27	0.09

Table 2. Rate constants obtained for TcC.

T (°C)	*k* (4.65 – 5.9 min)	*k* (6.5-9.5 min)	*k* (12.5-25 min)
270	0.78	0.19	0.08
290	1.05	0.19	0.08
310	0.96	0.16	0.06
330	0.87	0.13	0.06
350	0.89	0.20	0.06
370	0.74	0.16	0.16

From the data in Tables 1 and 2, ln *k* values were calculated and are plotted as a function of the inverse of the temperature (1/*T*) for the three time intervals to obtain Arrhenius parameters. Fig. 4 shows the plots for TcA. For TcC the results are shown in Supplementary data.

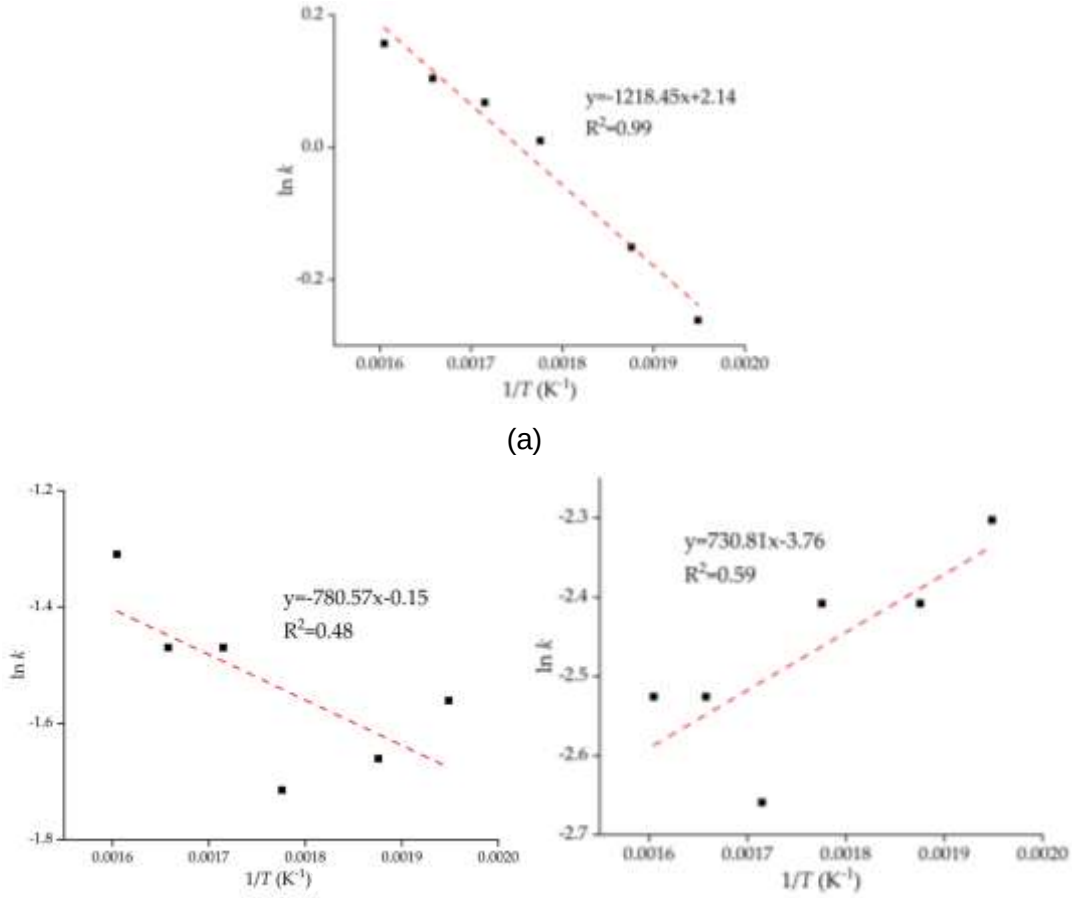

Fig. 4. Arrhenius plots of TcA for three different time regions (a) 4.4 – 5.7 min, (b) 6.2 – 11.3 min and (c) 12.5 – 25 min.

The R^2 values on each of the plots in Fig. 4 represent the accuracies of possible linear fits and hence reflect the credibility of derived activation energies and from application of the Guggenheim method in general. It can be seen that only the plot for TcA for the time interval of 4.4 – 5.7 min gave $R^2 \geq 0.98$ leading to an E_a value of 10.1 kJ/mol. The Arrhenius plots for the second and third time intervals have low regression coefficients. Thus, there was a little point in analysing the data further. As for TcC, the Arrhenius plots are meaningless, possibly reflecting a more complex mechanism of decomposition for this lignin as suggested previously in the Introduction (Patwardhan et al., 2011) and that the assumed first order reaction implicit in the Guggenheim method simply does not apply to these reactions beyond the very earliest stage (i.e. the stage explored using the initial rate method).

Unfortunately, no other reports exist of analysis of the kinetics of lignin decomposition using Guggenheim's method and so, the data obtained in this work cannot be easily compared. Generally, though, the value of E_a of 10.1 kJ/mol obtained here for the thermal decomposition of TcA between 4.4 and 5.7 min, is significantly lower than values reported in the literature for comparable lignins. Generally, most activation energy values reported for lignin pyrolysis are within the range of 60 - 90 kJ/mol (Ferdous et al., 2002; Rao and Sharma, 1998; Nunn et al., 1985), although some much higher values between 140 and 291 kJ/mol have been presented (Avni and Coughlin, 1985; Mani et al., 2009; Culebras et al., 2018; Svenson et al., 2004). The differences between calculated kinetic parameters reported by others are most likely due to the different types of lignin used, the experimental conditions under which pyrolyses were carried out, and the methods of calculation employed along with their implicit assumptions.

3.3 Isothermal kinetic study using Avrami-Erofeev method

As mentioned in the introduction, assuming the thermal degradation of lignin to be a first-order reaction throughout is almost certainly not appropriate because of the known inhomogeneous chemical structure of lignin. Hence, the Avrami-Erofeev model, from which reaction order can be calculated, has also been used in this work. This method is commonly used for complex processes and assumes that

$$[-\ln(1-\alpha)]^{\frac{1}{n}} = kt \qquad (14)$$

where n represents the order of reaction, *k* is the rate constant and α is the conversion value. Taking logarithms of both sides of Eq. (14) gives Eq. (15):

$$\ln[-\ln(1-\alpha)] = n\ln t + \ln k \qquad (15)$$

By plotting $\ln[-\ln(1-\alpha)]$ as a function of $\ln t$, the slope n and the intercept $\ln k$ can be obtained.

The plot for TcA pyrolyzed at 260 °C is presented as an example below in Fig. 5 (a). This plot is largely linear with a high R^2 value of 0.99. The R^2 value of the plot for TcC is also over 0.98, which indicates the consistency of the data with respect to the Avrami Eq.

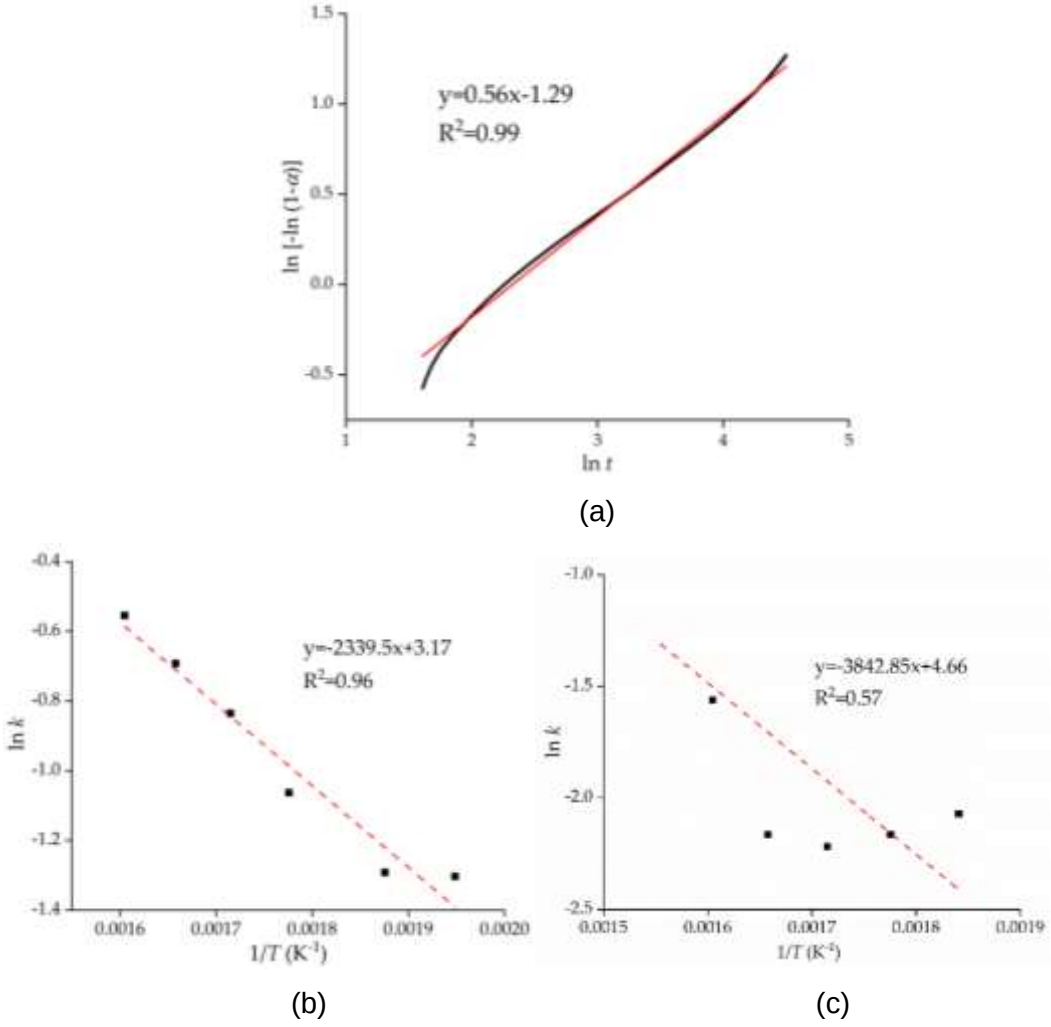

Fig. 5. (a) The plot of ln [-ln (1-α)] vs. ln *t* at 260°C for TcA, and Arrhenius plots of (b) TcA and (c) TcC under nitrogen.

Table 3. Values of n and ln k for TcA and TcC at different degradation temperatures.

Temp	TcA		TcC	
(°C)	ln *k*	*n*	ln *k*	*n*
240	-1.303	0.541		
260	-1.2915	0.5558		
270			-2.0706	0.6501
290	-1.0633	0.5161	-2.1641	0.666
310	-0.8356	0.4641	-2.2177	0.679

330	-0.6925	0.4312	-2.1633	0.7364
350	-0.5546	0.4076	-1.5612	0.6347
370			-0.8417	0.4556

Table 3 lists the kinetic data obtained from the Avrami plots. Based on the Arrhenius Eq. (9), plots of ln *k* against 1/*T* were constructed and are shown in Fig. 5 (b, c).

As can be seen in Fig. 5 (b, c)), the data for TcA falls close to a straight line with a regression coefficient, $R^2 = 0.96$, but the data for TcC is too poor a fit with R^2 of only 0.57. This might be due to a more complex decomposition mechanism for TcC owing to its more complex structure containing hydroxypropyl substituents, which have been shown to generate acetone (Culebras et al., 2018). This more complex degradation may also have been reflected in the non-sensible results using the Guggenheim method for TcC observed above. Additionally, the pyrolysis of lignin is considered to be a free radical process involving several series and parallel reactions (Zhang et al., 2021) which may be reflected in the various orders of reaction reported in Table 3. The E_a of TcA was calculated to be 19.4 kJ/mol, which is similar to the value of 12.4-42.6 kJ/mol from Klason lignin, which Pasquali et al. (1997) obtained using the Avrami method.

3.4 Non-isothermal kinetic analysis

Kinetic parameters for lignin decomposition have also been obtained using Kissinger's method (Kissinger, 1957) applied to a series of dynamic TGA experiments in which rates of mass loss are plotted as a function of temperature (so-called DTG curves) during the course of a predetermined heating rate. In this method, by plotting the logarithm of $\frac{\beta}{{T_m}^2}$ against $\frac{1}{T_m}$, the activation energy E_a may be calculated from the slope ($= -\frac{E_a}{R}$) of the linear regression curves, where β is the heating rate and T_m is the temperature at highest peak point in differential thermogravimetric (DTG) plots.

The order of reaction, n is determined by Eq. (16),

$$S = 0.63n^2 \qquad (16)$$

where the shape index S is obtained from Eq. (17) in which $\left(\frac{d^2\alpha}{dT^2}\right)_L$ and $\left(\frac{d^2\alpha}{dT^2}\right)_R$ represent the slopes of the DTG curve on left and right side of the highest peak point in DTG plots.

$$S = \left|\frac{\left(\frac{d^2\alpha}{dT^2}\right)_L}{\left(\frac{d^2\alpha}{dT^2}\right)_R}\right| \qquad (17)$$

After deriving the values of n and E_a, the pre-exponential factor A can be obtained from Eq. (5). According to Kissinger's method, the activation energy and pre-exponential factor are obtained for the whole conversion period, which can provide an overall average picture of the degradation process (Kissinger, 1957). This method has been shown to be the best one for kinetic parameter determination for biomass pyrolysis by Abdelouahed et al. (Abdelouahed et al, 2017).

Fig. 6 (a, b) depicts the DTG curves of TcA and TcC at six different heating rates (5, 10, 20, 50, 75 and 100 ^{o}C/min, respectively). The main degradation region of both lignins occurs between 250 and 550 ^{o}C. With an increase in heating rate, the highest peak of the curve, as well as the temperature of the maximum rate of degradation, shift to higher temperatures as seen from the data in Table 4 owing to the influence of the changing mass and of the heat transfer characteristics of the samples, which change with temperature (Tanoue et al., 2020).

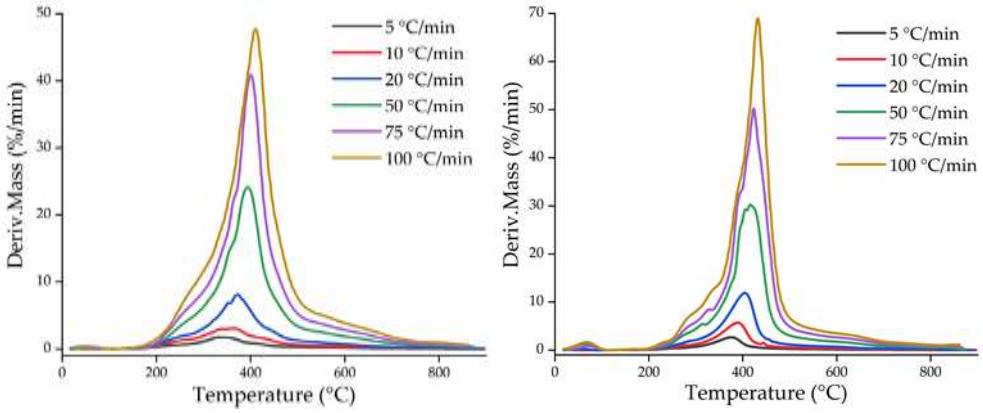

(a) (b)

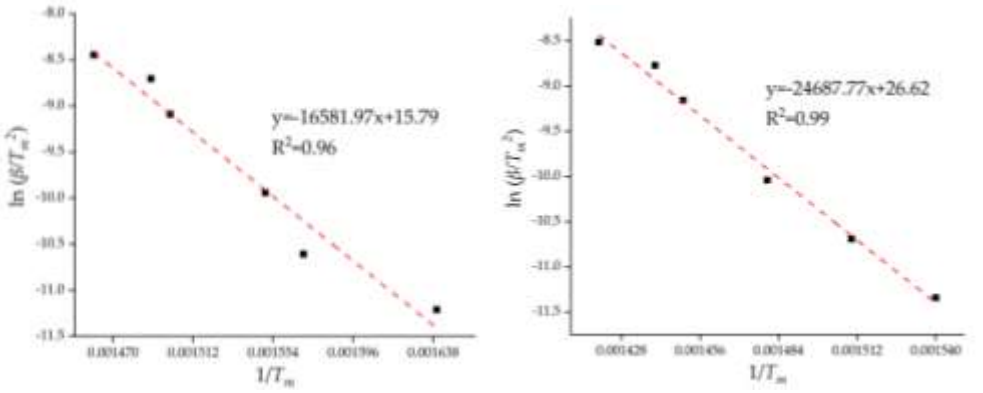

(c) (d)

Fig. 6. (a, b) DTG curves for TcA (a) and TcC (b) at various heating rates under nitrogen, and plots of ln (β/T_m^2) vs. $1/T_m$ for (c) TcA and (d) TcC. The line is the linear regression of the data points.

Application of Kissinger's method to the data leads to Fig. 6 (a, b) which shows plots of $\ln\left(\frac{\beta}{T_m{}^2}\right)$ against $\frac{1}{T_m}$ for the two lignins. These plots are linear with correlation coefficients, R^2, of 0.96 and 0.99, respectively, which there are indications of the credibility of the overall activation energy values obtained using Kissinger's model. Other kinetic parameters for TcA and TcC obtained from the TGA experiments are listed in Table 4.

Table 4. Kinetic parameters at the different heating rates for TcA and TcC under nitrogen.

β	TcA					TcC				
(°C/min)	T_{max} (°C)	S	n	E_a (kJ/mol)	A	T_{max} (°C)	S	n	E_a (kJ/mol)	A*
5	335	1.33	1.45			376	0.64	1.01		
10	363	1.1	1.32			390	0.87	1.18		
20	372	1.29	1.43			404	0.73	1.08		
50	393	1.2	1.38	137.9	1.3×10^9	415	0.74	1.08	205.3	1.4×10^{13}
75	400	1.03	1.27			422	1.01	1.27		
100	410	1.33	1.45			432	1.06	1.3		
Average	379	1.21	1.38			407	0.93	1.15		

Note: *Ideally A should have units s^{-1} if the reaction was wholly first order. Since this is not the case, A is expressed as unitless.

The shape indices (S) and reaction order (n) are similar at different heating rates for both lignins, which indicates that heating rate does not have an obvious impact on either of them. However, TcA has a higher average value (1.38) of reaction order than that (1.15) of TcC. As can be seen from Table 4, the derived activation energies E_a of TcA and TcC are 137.9 kJ/mol and 205.3 kJ/mol, respectively. Both E_a values are much higher than those calculated by the other three models under isothermal conditions, which is because with this method the value is an average for the overall pyrolysis process rather than for specific time periods in the isothermal methods. The values though are similar to those obtained for other lignins from other

non-isothermal experiments reported by Hu and Jiang (2020) (E_a = 51.2 - 264.8 kJ/mol) and Avni and Coughlin (1985) (E_a = 58.6 - 291.6 kJ/mol).

4. Discussion

The assumption of a first-order reaction for the initial stage (3 – 5 min) of the thermal decomposition (mass loss) of each lignin when applied to the analysis of dynamic TGA data (see Fig. 2 (b, c) has provided sensible activation energies: 39.0 ± 2.0 kJ/mol for TcA and 41.5 ± 1.4 kJ/mol for TcC. These are, however, much lower than the values of E_a (51.2 – 291.6 kJ/mol) obtained from other studies (Hu and Jiang, 2020; Avni and Coughlin, 1985; Ferdous et al., 2002; Mani et al., 2009, see Table 5), which considered the whole pyrolysis process. The mechanism of pyrolysis of lignin is considered to start with the cleavage of weak linkage bonds, leading to the removal of functional groups with low dissociation energies such as hydroxyl (−OH), methoxy (−OCH_3) and methyl (−CH_3) groups (Culebras et al., 2018; Klein and Virk, 1983). These groups are relatively easily eliminated in the initial pyrolysis process to produce a variety of gaseous products such as CO_2, CO, CH_4, alcohol within the temperature range of 166 - 274 ^oC (Culebras et al., 2018; Liu et al., 2008). Following the cleavage of ether linkages at higher temperatures, dimeric, phenolic, and oligomeric intermediates may also be released. E_a values in this stage are relatively low (Dussan et al., 2019). The low E_a value of 10.13 kJ/mol of TcA, which was obtained from Guggenheim's method under isothermal conditions also accords with this point, because the early pyrolysis period (4.4 – 5.7 min) was chosen for model analysis. Clearly, the assumption of first-order kinetics is not applicable to the whole mass-loss process for either lignin, thus no sensible kinetic parameters could be obtained. From the above discussion, it is reasonable to conclude, as expected, that first-order kinetics do not apply throughout the reactions occurring in the pyrolysis of lignin, but only for the initial stage, a limitation not explicitly acknowledged by previous workers.

Using Avrami's method, the overall reaction orders of TcA and TcC lignins at different temperatures were about 0.4 - 0.5 and 0.6 – 0.7, respectively, which is similar to that of Klason lignin reported by Pasquali and Herrera (Pasquali and Herrera, 1997, Table 5). This is possibly due to the gradually decreasing mass loss rates at longer periods in isothermal experiments, which approximate to zero order kinetics and which are probably mainly controlled by slow diffusion of previously liberated products from the residual char. However, non-linear Arrhenius plots from which no activation energies can be obtained mean that, in our view, the Avrami

approach throws no useful light on the kinetics and mechanisms of lignin decomposition, contrary to the reports of Pasquali and Herrera (Pasquali and Herrera, 1997).

According to the mechanistic studies in the literature, with an increase in temperature, aromatization within lignin may be further accelerated (Yang et al., 2020). The cleavage of C-C and C-H bonds will result in many more free radicals amongst the degradation products, enhancing the removal of those weakly bonded functional groups (Yang et al., 2020). At this stage, a higher E_a value would be required for the fracture of more functional groups, as well as for the rearrangement and repolymerisation or interaction of pyrolysis products. Therefore, a relatively high E_a may be expected when the decomposition is analysed over the whole pyrolysis reaction at different heating rates by Kissinger's method. This method yielded different results than those obtained from isothermal runs, in that both the average order of reaction and activation energy E_a obtained by non-isothermal TGA were higher than those obtained in the isothermal studies. There could be two reasons for this. Firstly, the TGA instrument cannot instantaneously heat up to the required isothermal temperature, resulting in a short non-isothermal period lasting for approximately the first three minutes of each isothermal run. At this stage, there may be partial bond fracture as well as loss of moisture. Secondly, while the subsequent initial degradation stages may follow first order kinetics, this cannot be assumed to be applicable to the later stages of lignin pyrolysis, given the structural complexity of lignin

Thus it is worth comparing the E_a values derived in this work with those from other studies, as data presented in Table 5. From isothermal experiments, the organosolv lignin (TcA) and hydroxypropyl-modified lignin (TcC) have overall E_a of 39.0 and 41.5 kJ/mol for the initial mass-loss stages as previously mentioned, which although quite low, are similar to those reported by some other researchers in the literature (Pasquali and Herrera, 1997; Chan and Krieger, 1981; Ojha et al., 2017). Non-isothermal methods give, for the organosolv (TcA) and hydroxypropyl-modified (TcC) lignins, overall E_a of 137.9 kJ/mol and 205.3 kJ/mol, respectively, which are similar to those reported for Kraft lignin by Ferdous et al (2002) (80-158 kJ/mol) and Alcell lignin by Mani et al (2009) (83-195 kJ/mol).

Table 5. Kinetic parameters for the pyrolysis of lignin from literature

Type of lignin	Pyrolysis conditions	Kinetic model	Kinetic parameters			Reference
			E_a (kJ/mol)	A (min^{-1})	n	
Klason	Iso; 226 – 435 ^{o}C; 85 min	AE	12.5 - 42.6	-	0.5	Pasquali and Herrera (1997)

Alkali	Iso; 400 – 700 ^{o}C; 30 s	1st-order 1D diffusion 2D diffusion AE	23 23 8.9 21.4	3.9 ×10^{2} 1.6 ×10^{2} 1.1 2.4 ×10^{2}	-	Ojha et al. (2017)
Kraft	Microwave; 1.5 kW; 5 min	1st-order	25.2	4.7×10^{2}	1	Chan and Krieger (1981)
Aspen	N-Iso; RT – 800 ^{o}C; 0.5 – 100 ^{o}C/min	Guassian	58.6–291.6	2.7×10^{8}	1.1	Avni and Coughlin (1985)
Rice hull	N-Iso; RT - 900 ^{o}C; 3 – 100 ^{o}C/min	4-lump	34	5.5	1	Teng and Wei (1998)
Rice husk	N-Iso; RT – 500 ^{o}C, 20 ^{o}C/min	n^{th}-order	67 (n=1) 71 (n=2)	5.4 × 10^{4} 2.1 × 10^{5}	1 2	Rao and Sharma (1998)
Kraft	N-Iso; RT - 900 ^{o}C; 5 – 15 ^{o}C/min	DEAM	80-158	6.2×10^{11}-9.3×10^{22}	1	Ferdous et al. (2002)
7 types (ABL, EBL, EML, BLL, APL, ACL, CECL)	N-Iso; RT - 900 ^{o}C;, 10, 20 and 40 ^{o}C/min	St-K	51 – 265	1.4 ×10^{2} –1.1 ×10^{5}	1	Hu and Jiang (2020)
PL, MWL	N-Iso; RT - 800 ^{o}C;, 20 ^{o}C/min	DG-DEAM	135.8 (PL) 148.8 (MWL)	-	-	Wang et al. (2014)
De-alkaline	N-Iso; 105 – 800 ^{o}C; 1, 5, 20, 40 ^{o}C/min	IPR	30 – 673	4.8 x 10^{-3} – 1.1 x 10^{32}	-	Chen et al. (2020)
Alkali	N-Iso; RT – 900 ^{o}C; 10, 40 and 70 ^{o}C/min	Friedman KAS OFW	117 110 191	6.8 x 10^{16} 1.2 x 10^{36} 1.7 x 10^{16}	1	Dash et al. (2022)
Alkali	N-Iso; RT – 600 ^{o}C; 10, 20, 30 and 40 ^{o}C/min	n^{th}-order	47 (n=1) 61 (n=2) 78 (n=3)	3.7 1.1 ×10^{2} 5.5 x 10^{3}	1 2 3	Bu et al. (2016)
Alkaline (A), De-alkaline (D)	N-Iso; RT – 600 ^{o}C; 5 ^{o}C/min	Friedman	33 – 143 (A) 87 – 133 (D)	-	-	Damayanti and Wu (2017)
Klason	N-Iso; RT - 650 ^{o}C;, 5, 10 and 20 ^{o}C/min	KAS OFW MC-DEAM	82 – 244 86 – 243 169 – 209	-	-	Kristanto et al. (2022)
Alcell	N-Iso; RT - 700 ^{o}C;, 5, 10 and 15 ^{o}C/min	DEAM	83-195	-	1	Mani et al. (2009)

Note:
ABL = acid-extracted birch lignin; EBL = ethanol-extracted birch lignin; EML = ethanol-extracted maple lignin; BLL = black liquor lignin; APL = acid-extracted pine lignin; ACL = acid-extracted corn stalk lignin; CECL = cellulolytic enzyme corn stalk lignin; PL = pyrolytic lignin; MWL = milled wood lignin.# Iso = isothermal; N-Iso = non-isothermal; RT = room temperature.
AE = Avrami-Erofeev model; St-K = combined Starink and Kissinger model; DEAM = distributed activation energy model; KAS = Kissinger-Akahira-Sunose model; OFW = Ozawa-Flynn-Wall model; DG-DEAM = Double-Gaussian distributed activation energy mode; MC-DEAM = multi-component distributed activation energy model; IPR = Independent parallel reaction.

Kissinger's method of analysis, gives orders of reaction for TcA and TcC pyrolyses that are both greater than 1, indicating that the thermal decomposition of lignin is not a simple first order process. The complex structure of lignin, which contains different functional groups and types of linkage, means that different reactions will occur over different ranges of temperature, with those of lowest activation energy occurring first. Moreover, the fractional orders of reaction can only arise in a complex chemical process, such as a free radical chain reaction. The products of these initial reactions will further add to the complexity of subsequent reactions. In addition, different lignins from different natural origins and extracted by different processes will display different pyrolysis behaviours as a consequence of their decomposing by different mechanisms.

While the three isothermal TGA methods used in this study did not provide any useful information regarding detailed mechanisms of pyrolysis of two different lignin types, similar but very low E_a values of both TcA and TcC indicate that they behave similarly in early stages of pyrolysis. Different parameters obtained for the two lignins indicate that the thermal decomposition of the two lignins, although superficially similar (Fig. 1 (a)), follow significantly different paths at the molecular level. In both cases, on heating, there is competition between thermodynamic and kinetic factors leading to structurally different products, as explained in details elsewhere (Culberas et al., 2018b). The higher E_a value for TcC than for TcA for the overall pyrolysis process obtained from the non-isothermal method indicates a higher thermal stability for TcC, relative to that of TcA, which could be beneficial for thermal stabilisation and carbonisation processes in carbon fibre production and which is consistent with results of some of our ongoing (Muthuraj et al., 2020) and unpublished work in this area. For this both lignins were melt blended with a bio-based polyamide, PA 1010, and extruded into fibres. These precursor fibres were then thermally stabilised in an oven at 0.25 ^{o}C/min heating rate to 180 and 250 ^{o}C for 1 and 2 h, respectively (Muthuraj et al 2021). The thermostabilised fibres were subsequently carbonised by heating to 1000^{o}C at 20^{o}C/min for 3 minutes under nitrogen

atmosphere. The lower E_a value of TcA, could also be beneficial for activated carbon formation, in which char formation and its activation for increased porosity are important factors (Ouyang et al., 2020; Liao et al., 2022), and which has been demonstrated in our ongoing work and will be presented in a forthcoming publication.

5. Conclusions

Activation energies and pre-exponential factors for lignin pyrolysis obtained from TGA data using different analytical kinetic models, depend on method of analysis and lignin type. Only the first stage of decomposition is truly first order, a fact not appreciated in some previous work, yielding an activation energy of the size expected for breakage of the weakest chemical bonds. Kinetic parameters obtained for later stages confirm that pyrolysis of lignin is a complex process probably involving sequential and parallel reactions. These data are of significance when considering the potential of lignins as precursors for carbon fibres, activated carbons, and biofuels.

Acknowledgments

This research was funded by the Bio- Based Industries Joint Undertaking under the European Union's Horizon 2020 research and innovation programme under Grant Agreement No. 720707. The authors wish to acknowledge Gianmarco Panzetti for initial experimental studies (see Culebras et al., 2018b)

References

Abdelouahed, L., Leveneur, S., Vernieres-Hassimi, L., Balland, L., Taouk, B., 2017. Comparative investigation for the determination of kinetic parameters for biomass pyrolysis by thermogravimetric analysis. J. Therm. Anal. Calorim. 129, 1201–1213. https://doi.org/10.1007/s10973-017-6212-9

Avni, E., Coughlin, R.W., 1985. Kinetic analysis of lignin pyrolysis using non-isothermal TGA data. Thermochim. Acta 90, 157–167. https://doi.org/10.1016/0040-6031(85)87093-3.

Brebu, M., Vasile, C., 2010. Thermal degradation of lignin - A review. Cellul. Chem. Technol. 44, 353–363.

Bu, Q., Lei, H., Qian, M., Yadavalli, G., 2016. A thermal behavior and kinetics study of the catalytic pyrolysis of lignin. RSC Adv. 6, 100700–100707. https://doi.org/10.1039/c6ra22967k.

Chan, R.W.-C., Krieger, B.B., 1981. Kinetics of dielectric-loss microwave degradation of polymers: Lignin. J. Appl. Polym. Sci. 26, 1533–1553. https://doi.org/10.1002/app.1981.070260510.

Chen, W.-H., Eng, C.F., Lin, Y.-Y., Bach, Q.-V., 2020. Independent parallel pyrolysis kinetics of cellulose, hemicelluloses and lignin at various heating rates analyzed by evolutionary computation. Energy Convers. Manag. 221, 113165. https://doi.org/10.1016/j.enconman.2020.113165.

Coats, A.W., Redfern, J.P., 1964. Kinetic parameters from thermogravimetric data. Nature 201, 68–69. https://doi.org/10.1038/201068a0.

Culebras, M., Beaucamp, A., Wang, Y., Clauss, M.M., Frank, E., Collins, M.N., 2018a. Biobased structurally compatible polymer blends based on lignin and thermoplastic elastomer polyurethane as carbon fiber precursors. ACS Sustain. Chem. Eng. 6, 8816–8825. https://doi.org/10.1021/acssuschemeng.8b01170.

Culebras, M., Sanchis, M.J., Beaucamp, A., Carsí, M., Kandola, B.K., Horrocks, A.R., Panzetti, G., Birkinshaw, C., Collins, M.N., 2018b. Understanding the thermal and dielectric response of organosolv and modified kraft lignin as a carbon fibre precursor. Green Chem. 20, 4461–4472. https://doi.org/10.1039/c8gc01577e.

Damayanti, Wu, H.S., 2017. Pyrolysis kinetic of alkaline and dealkaline lignin using catalyst. J. Polym. Res. 25. https://doi.org/10.1007/s10965-017-1401-6

Dash, S., Thakur, S., Bhavanam, A., Gera, P., 2022. Catalytic pyrolysis of alkaline lignin: A systematic kinetic study. Bioresour. Technol. Rep. 18, 101064. https://doi.org/10.1016/j.biteb.2022.101064.

Dussan, K., Dooley, S., Monaghan, R.F.D., 2019. A model of the chemical composition and pyrolysis kinetics of lignin. Proc. Combust. Inst. 37, 2697–2704. https://doi.org/10.1016/j.proci.2018.05.149.

Effendi, A., Gerhauser, H., Bridgwater, A. V. 2008. Production of renewable phenolic resins by thermochemical conversion of biomass: A review. Renew. Sust. Energ. Rev., 12(8), 2092–2116. https://doi.org/10.1016/j.rser.2007.04.008.

Ferdous, D., Dalai, A.K., Bej, S.K., Thring, R.W., 2002. Pyrolysis of lignins: Experimental and kinetics studies. Energy Fuels 16, 1405–1412. https://doi.org/10.1021/ef0200323.

Flynn, J.H., Wall, L.A., 1966. General treatment of the thermogravimetry of polymers. J. Res. Natl. Bur. Stand. A Phys. Chem. 70A (6), 487-523. https://doi.org/10.6028/jres.070a.043.

Freeman, E.S., Carroll, B., 1958. The application of thermoanalytical techniques to reaction kinetics: The thermogravimetric evaluation of the kinetics of the decomposition of

calcium oxalate monohydrate. J. Phys. Chem. 62, 394–397. https://doi.org/10.1021/j150562a003.

Friedman, H.L., 2007. Kinetics of thermal degradation of char-forming plastics from thermogravimetry. Application to a phenolic plastic. J. Polym. Sci., Polym. Symp. 6, 183–195. https://doi.org/10.1002/polc.5070060121.

Gellerstedt, G., Henriksson, G., 2008. Lignins: Major sources, structure and properties, in: Belgacem, M.N., Gandini, A. (Eds.), Monomers, Polymers and Composites from Renewable Resources. Elsevier, Amsterdam, pp 201–224. https://doi.org/10.1016/b978-0-08-045316-3.00009-0.

Guggenheim, E.A., 1926. XLVI. On the determination of the velocity constant of a unimolecular reaction. Lond. Edinb. Dublin Philos. Mag. J. Sci. 2, 538–543. https://doi.org/10.1080/14786442608564083.

Hu, J., Jiang, X., 2020. Pyrolysis characteristics and kinetics of lignin: effect of starting lignins. Energy Sources A: Recovery Util. Environ. Eff. 1–13. https://doi.org/10.1080/15567036.2020.1860160.

Jiang, G., Nowakowski, D.J., Bridgwater, A.V., 2010. A systematic study of the kinetics of lignin pyrolysis. Thermochim. Acta 498, 61–66. https://doi.org/10.1016/j.tca.2009.10.003.

Kissinger, H.E., 1957. Reaction Kinetics in Differential Thermal Analysis. Anal. Chem. 29, 1702–1706. https://doi.org/10.1021/ac60131a045.

Klein, M.T., Virk, P.S., 1983. Model pathways in lignin thermolysis. 1. Phenethyl phenyl ether. Ind. Eng. Chem. 22, 35–45. https://doi.org/10.1021/i100009a007.

Kristanto, J., Daniyal, A.F., Pratama, D.Y., Bening, I.N.M., Setiawan, L., Azis, M.M., Purwono, S., 2022. Kinetic Study on the slow pyrolysis of isolated cellulose and lignin from teak sawdust. Thermochim. Acta 711, 179202. https://doi.org/10.1016/j.tca.2022.179202.

Kumar, M., Upadhyay, S.N., Mishra, P.K., 2019. A comparative study of thermochemical characteristics of lignocellulosic biomasses. Bioresour. Technol. Rep. 8, 100186. https://doi.org/10.1016/j.biteb.2019.100186.

Li, B., Zhang, X., Su, R., 2002. An investigation of thermal degradation and charring of larch lignin in the condensed phase: the effects of boric acid, guanyl urea phosphate, ammonium dihydrogen phosphate and ammonium polyphosphate. Polym. Degrad. Stab. 75, 35–44. https://doi.org/10.1016/s0141-3910(01)00202-6.

Liao, Z., Zhu, Y.-H., Sun, G.-T., Qiu, L., Zhu, M.-Q., 2022. Micromorphology control of the lignin-based activated carbon and the study on the pyrolysis and adsorption kinetics. Ind. Crops Prod. 175, 114266. https://doi.org/10.1016/j.indcrop.2021.114266.

Liu, Q., Wang, S., Zheng, Y., Luo, Z., Cen, K., 2008. Mechanism study of wood lignin pyrolysis by using TG–FTIR analysis. J. Anal. Appl. Pyrolysis. 82, 170–177. https://doi.org/10.1016/j.jaap.2008.03.007.

Lupoi, J.S., Singh, S., Parthasarathi, R., Simmons, B.A., Henry, R.J., 2015. Recent innovations in analytical methods for the qualitative and quantitative assessment of lignin. Renew. Sust. Energ. Rev. 49, 871–906. https://doi.org/10.1016/j.rser.2015.04.091.

Mani, T., Murugan, P., Mahinpey, N., 2009. Determination of distributed activation energy model kinetic parameters using simulated annealing optimization method for nonisothermal Pyrolysis of Lignin. Ind. Eng. Chem. Res. 48, 1464–1467. https://doi.org/10.1021/ie8013605.

Muthuraj, R., Horrocks, A.R., Kandola, B.K., 2020. Hydroxypropyl-modified and organosolv lignin/bio-based polyamide blend filaments as carbon fibre precursors'. J. Mater. Sci. 55, 7066–7083. https://doi.org/10.1007/s10853-020-04486-w.

Muthuraj, R., Hajee, M., Horrocks, A.R., Kandola, B.K., 2021. Effect of compatibilizers on lignin/bio-polyamide blend carbon precursor filament properties and their potential for thermostabilisation and carbonisation. Polym. Test. 95, 107133. https://doi.org/10.1016/j.polymertesting.2021.107133.

Narnaware, S.L., Panwar, N.L., 2022. Kinetic study on pyrolysis of mustard stalk using thermogravimetric analysis. Bioresour. Technol. Rep. 17, 100942. https://doi.org/10.1016/j.biteb.2021.100942.

Nunn, T.R., Howard, J.B., Longwell, J.P., Peters, W.A., 1985. Product compositions and kinetics in the rapid pyrolysis of milled wood lignin. Ind. Eng. Chem. Process. 24, 844–852. https://doi.org/10.1021/i200030a054.

Ojha, D.K., Viju, D., Vinu, R., 2017. Fast pyrolysis kinetics of alkali lignin: Evaluation of apparent rate parameters and product time evolution. Bioresour. Technol. 241, 142–151. https://doi.org/10.1016/j.biortech.2017.05.084.

Ouyang, J., Zhou, L., Liu, Z., Heng, J.Y.Y., Chen, W., 2020. Biomass-derived activated carbons for the removal of pharmaceutical mircopollutants from wastewater: A review. Sep. Purif. Technol. 253, 117536. https://doi.org/10.1016/j.seppur.2020.117536.

Ozawa, T., 1965. A New Method of Analyzing Thermogravimetric Data. Bull. Chem. Soc. Jpn. 38, 1881–1886. https://doi.org/10.1246/bcsj.38.1881.

Pasquali, C.E.López., Herrera, H., 1997. Pyrolysis of lignin and IR analysis of residues. Thermochim. Acta 293, 39–46. https://doi.org/10.1016/s0040-6031(97)00059-2.

Patwardhan, P.R., Brown, R.C., Shanks, B.H., 2011. Understanding the fast pyrolysis of lignin. Chem. Sus. Chem. 4, 1629–1636. https://doi.org/10.1002/cssc.201100133

Ramiah, M.V., 1970. Thermogravimetric and differential thermal analysis of cellulose, hemicellulose, and lignin. J. Appl. Polym. Sci. 14, 1323–1337. https://doi.org/10.1002/app.1970.070140518.

Rao, T.Rajeswara., Sharma, A., 1998. Pyrolysis rates of biomass materials. Energy 23, 973–978. https://doi.org/10.1016/s0360-5442(98)00037-1.

Saddawi, A., Jones, J.M., Williams, A., Wójtowicz, M.A., 2009. Kinetics of the thermal decomposition of biomass. Energy Fuels 24, 1274–1282. https://doi.org/10.1021/ef900933k.

Solomons, T.W.G., Fryhle, C.B., Snyder, S.A., 2017. Organic Chemistry. John Wiley & Sons, Inc, Hoboken, New Jersey.

Suhas, P., Carrott, M., Ribeiro Carrott, M.M.L. 2007. Lignin – from natural adsorbent to activated carbon: A review. Bioresour. Technol. 98 (12), 2301-2312. https://doi:10.1016/j.biortech.2006.08.008.

Svenson, J., Pettersson, J.B.C., Davidsson, K.O., 2004. Fast pyrolysis of the main components of Birch wood. Combust. Sci. Technol. 176, 977–990. https://doi.org/10.1080/00102200490428585.

Tanoue, K., Hikasa, K., Hamaoka, Y., Yoshinaga, A., Nishimura, T., Uemura, Y., Hideno, A., 2020. Heat and mass transfer during lignocellulosic biomass torrefaction: Contributions from the major components - cellulose, hemicellulose and lignin. Processes 8, 959. https://doi.org/10.3390/pr8080959.

Teng, H., Wei, Y.-C., 1998. Thermogravimetric studies on the kinetics of rice hull pyrolysis and the Influence of water treatment. Ind. Eng. Chem. Res. 37, 3806–3811. https://doi.org/10.1021/ie980207p.

Wang, S., Lin, H., Ru, B., Sun, W., Wang, Y., Luo, Z. 2014. Comparison of the pyrolysis behavior of pyrolytic lignin and milled wood lignin by using TG–FTIR analysis. J. Anal. Appl. Pyrol. 108, 78–85. https://doi.org/10.1016/j.jaap.2014.05.014

Wang, X., Hu, M., Hu, W., Chen, Z., Liu, S., Hu, Z., Xiao, B., 2016. Thermogravimetric kinetic study of agricultural residue biomass pyrolysis based on combined kinetics. Bioresour. Technol. 219, 510–520. https://doi.org/10.1016/j.biortech.2016.07.136

Yang, J., Wang, X., Shen, B., Hu, Z., Xu, L., Yang, S., 2020. Lignin from energy plant (Arundo donax): Pyrolysis kinetics, mechanism and pathway evaluation. Renew. Energy. 161, 963–971. https://doi.org/10.1016/j.renene.2020.08.024.

Zhang, D., Zeng, J., Liu, W., Qiu, X., Qian, Y., Zhang, H., Yang, Y., Liu, M., Yang, D., 2021. Pristine lignin as a flame retardant in flexible PU foam. Green Chem. 23, 5972–5980. https://doi.org/10.1039/d1gc01109j.

Supplementary data

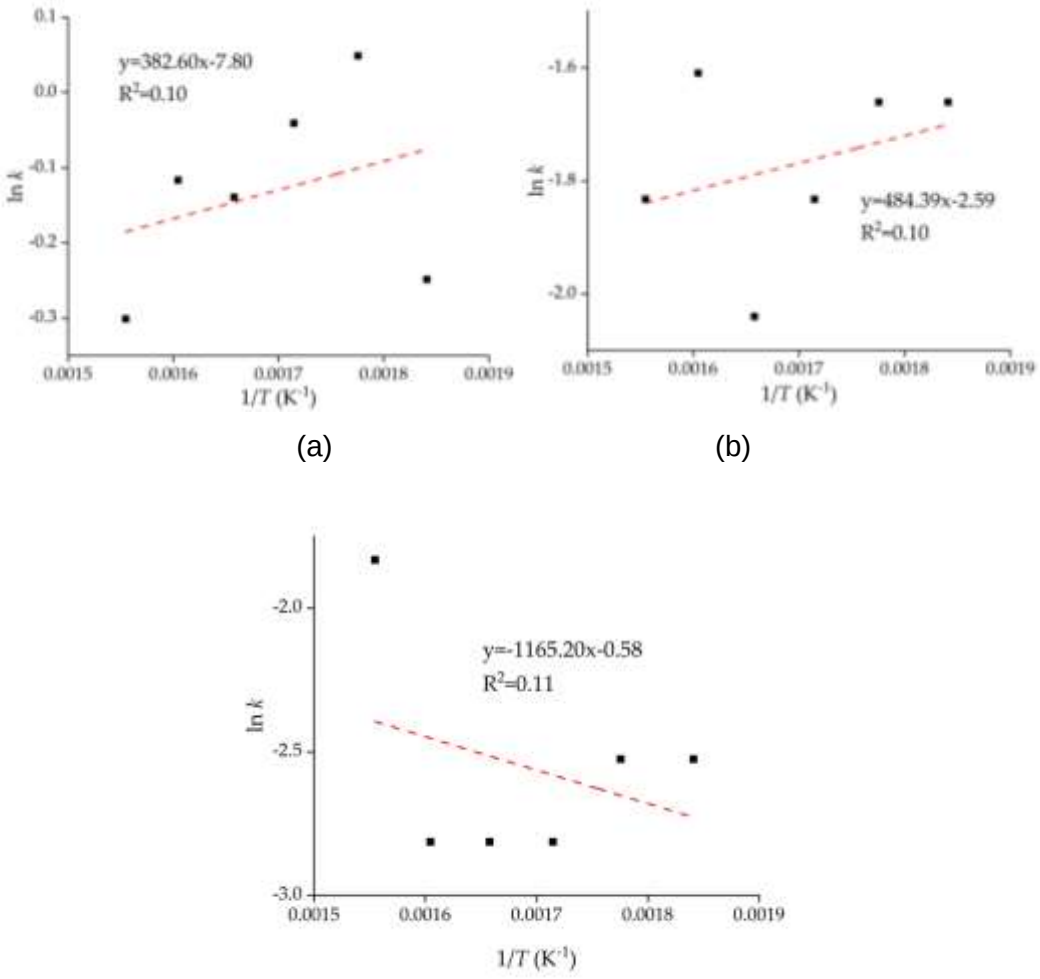

Figure S1. Arrhenius plots of TcC for three different time regions (a) 4.65 – 5.9 min, (b) 6.5 – 9.5 min and (c) 12.5-25 min.